Available online at www.sciencedirect.com

SciVerse ScienceDirect

Ceramics International 38 (2012) 4009–4016

CERAMICS INTERNATIONAL

www.elsevier.com/locate/ceramint

Synthesis and optical properties of $Ce_{0.95}Pr_{0.05-x}M_xO_2$ (M = Mn, Si) as potential ecological red pigments for coloration of plastics

L. Sandhya Kumari [a], P. Prabhakar Rao [a,*], S. Sameera [a], Peter Koshy [b]

[a] *Materials and Minerals Division, National Institute for Interdisciplinary Science and Technology, Thiruvananthapuram 695 019, India*
[b] *Mount Zion College of Engineering for Women, Chengannur 689 521, India*

Received 13 December 2011; received in revised form 12 January 2012; accepted 20 January 2012
Available online 28 January 2012

Abstract

Ecological red pigments $Ce_{0.95}Pr_{0.05-x}M_xO_2$ (M = Mn, Si) have been synthesized by conventional solid-state route and characterized by X-ray diffractometer, scanning electron microscope and UV–vis spectroscopy. Mn^{4+}/Si^{4+} was incorporated into the CeO_2–PrO_2 system to tune the color properties of the pigments by shifting the optical absorption edge. Si^{4+} substitution blue shifts the absorption edge of Pr-doped ceria and shows bright reddish brown color. Mn^{4+} substitution stabilizes the absorption edge and exhibits dark brown hue. The coloring mechanism is based on the shift of charge transfer band of CeO_2 to higher wavelength by co-substitution of Pr^{4+} and tetravalent metal ions in ceria. Si co-doped pigments possess smaller particles and hence exhibit more lightness compared to Mn co-doped samples. The reddish brown pigments exhibit very good coloring performance in polymer matrix. These $Ce_{0.95}Pr_{0.05-x}M_xO_2$ (M = Mn, Si) pigments have potential to be used as ecological red pigments for coloration of plastics.

Keywords: A. Powders: solid state reaction; B. Spectroscopy; C. Optical properties; D. CeO_2; Coloration of plastics

1. Introduction

The search for new ceramic pigments is now a high-priority field in the ceramics industry because of the scarce variety of existing ones and the limitation imposed on their use by the current technological and ecological requirements [1,2]. The rare earth oxides, which are believed to be less toxic compared with transition metal ions, have a bright appearance and have potential to form ceramic colors. Research in the fields of ceramic pigments is oriented toward the enlargement of the chromatic set of colors together with an increased thermal and chemical stability. Pigments based on cerium dioxide are lesser known and represent only a small, but an important range of inorganic pigments. As pigments of red to orange hue, sulfides of Ce^{3+} ($4f^15d^0$) ions such as γ-Ce_2S_3 and its alkali-metal derivatives γ-$Ce_{2-x}A_{3x}S_3$ (A = alkali) have been proposed [3–5]. Pr-doped ceria pigments [6] give various pink-orange to red-brown hues, depending on the quantity of praseodymium, synthesis conditions, calcinations temperature [7–9]. It is further studied by admixture of various lanthanides like La_2O_3, Sm_2O_3, Nd_2O_3 and Gd_2O_3 [10–13]. However, the serious problem associated with these pigments is lack of thermal stability due to reduction of Ce(IV) oxide to Ce(III) oxide accompanied by releasing oxygen and the color tends to orange [14]. Hence, the above investigations have not lead to improve the red hue of the pigment to form a viable alternate to the traditional toxic red pigments. Terbium-doped ceria prepared through classical and non-conventional co-precipitation routes as environmentally friendly reddish ceramic pigments were investigated for the optimal composition and synthesis methods to get very nice reddish colorations [15].

CeO_2 is a fluorite-structured oxide where fcc packed Ce^{4+} ions are surrounded by eight oxygens, occupying alternate centers of tetrahedral cavities in the fcc lattice [16], that can form extensive solid solutions with a variety of alien cations while retaining the fluorite crystal structure. Ln–CeO_2 (Ln = Pr, Tb, Eu) and M–CeO_2 solid solutions M = Cr or In, have been reported as low-toxicity red ceramic pigments [16]. According to Jørgensen and Rittershaus [17] the red color of the praseodymium-doped samples is related to a charge-transfer

* Corresponding author. Tel.: +91 471 2515311; fax: +91 471 2491712.
E-mail address: padala_rao@yahoo.com (P.P. Rao).

0272-8842/$36.00
doi:10.1016/j.ceramint.2012.01.057

band due to an electron transfer from the ligand orbitals to the praseodymium cation. New safer inorganic red pigments with improved color properties have been reported by our group by the co-substitution of Zr and/or Sn in $Ce_{0.95}Pr_{0.05}O_2$ system [18]. It is well known in the literature that small amounts of tetravalent ions, i.e. Zr^{4+}, Hf^{4+}, Ti^{4+}, Si^{4+}, etc., are normally introduced into the ceria cubic structure to increase its thermal stability [19,20]. Substitution of transition metals like Cr, Mn, Fe in CeO_2 fluorite structure was also studied for OSC [21]. Optical properties of oxide materials based on silica and ceria have attracted attention. For example, cerium oxide doped with silicon is intensively investigated from the viewpoint of their potential applications as stable luminescent materials for phosphors, scintillators and detectors [22]. Optical absorption properties of the silica-coated CeO_2 materials have also been reported in recent works [23]. The high stability of CeO_2 and SiO_2 has been guaranteed for a long time as well as high durability against humidity, and therefore, they have potential to be new pigments [24]. Keeping these facts in mind, the main attention was focused on the pigment synthesis based on CeO_2 doped by small amounts of praseodymium and transition metal to achieve good red color characteristics in plastics. The main goal of this study is to understand relative influence of different counter ions in the optical properties of ceria based red pigments. In the present study, safer red pigments having the formula $Ce_{0.95}M_xPr_{0.05-x}O_2$, (M = Mn and Si, x ranges from 0 to 0.05) have been synthesized by a solid-state reaction of the respective oxides. These pigments were characterized for their structural and optical properties and the application of these pigments in a polymer matrix are highlighted.

2. Experimental procedure

2.1. Sample preparation

Compositions based on $Ce_{0.95}M_xPr_{0.05-x}O_2$, (M = Mn and Si, x ranges from 0 to 0.05) were prepared by the conventional ceramic route using corresponding oxides: CeO_2, MnO_2, SiO_2 and Pr_6O_{11} (99.99% purity Sigma Aldrich). Pr-doped CeO_2 is named as CP, Mn-substituted samples as Mn 1, Mn 2, Mn 3, Mn 4 and Mn 5 and Si-substituted compounds as Si 1, Si 2, Si 3, Si 4 and Si 5 with reference to mole percentage of substitution. (This nomenclature is followed herein after for ease of understanding.) The raw materials were mixed in the proper stoichiometric compositions and then homogenized by wet mixing with acetone in an agate mortar for 30 min. The homogeneous mixture was calcined in platinum crucibles in an electric furnace at a temperature of 1300 °C for 6 h. The heating of the furnace was programmed to increase the temperature initially at 10 °C/min up to 1000 °C and afterwards the heating rate was decreased to 5 °C/min up to 1300 °C. In order to ensure the completion of the reaction, the calcination process was repeated thrice for the same sample with intermittent grinding.

2.2. Sample characterization

Phase analysis of the colored samples was performed by X-ray powder diffraction using a Ni-filtered Cu Kα radiation with a powder X-ray diffractometer (XRD) (Philips X'pert Pro). Data were collected by a step-scanning from 10 to 90° 2θ. Phase identification was determined from these data. Particle morphological analysis of the powders was performed by means of a scanning electron microscope (SEM) (JEOL, JSM-5600LV). The high-resolution electron microscopy (HREM) was taken using transmission electron microscope (TEM) TECNAI $30G^2$ S-TWIN (FEI, The Netherlands) and micro chemical analysis of the samples were analyzed using energy dispersive spectrophotometer (EDS) attached with TEM. A small amount of finely powdered sample was dispersed in acetone medium by ultra-sonication, drop-cast on carbon-coated copper grids, and dried. The particle size distribution of the typical pigment samples (Mn 2 and Si 2) were investigated in water medium with calgon as the dispersing agent using the Laser Scattering Particle Size Distribution Analyzer (CILAS 930 Liquid). The samples were ultrasonically homogenized for 180 s during measurement and the signal was evaluated on the basis of Fraunhofer bending.

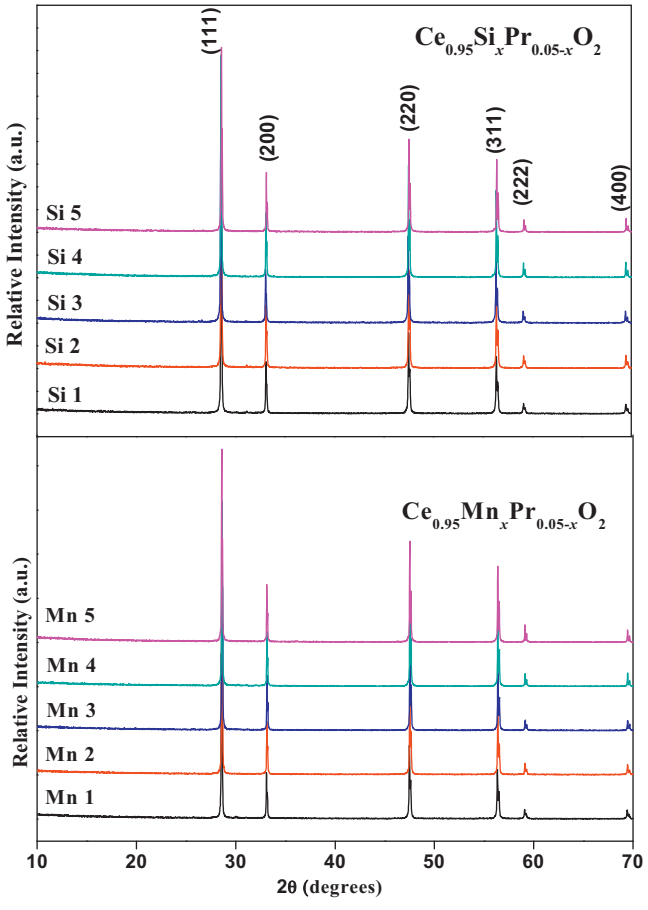

Fig. 1. XRD patterns of the $Ce_{0.95}M_xPr_{0.05-x}O_2$ (M = Mn and Si, x ranges from 0 to 0.05) pigments calcined at 1300 °C/6 h. All products are fluorite single-phase compounds with high crystallinity.

UV–vis spectroscopy and colorimetric study of the samples were carried out in a Shimadzu, UV-2450 spectrophotometer in the 380–780 nm wavelength range using barium sulfate as a reference. The band gap of the pigment samples was calculated from the absorption spectra using Shapiro's method by extrapolating the onset of absorption to the wavelength axis. The study of chromatic properties requires the use of an appropriate system to measure the color objectivity. The CIE-$L^*a^*b^*$ 1976 color scales were used for the assessment of the color properties of the pigment powders. In this system, L^* is the color lightness (L^* is 0 for black and L^* is 100 for white), a^* is the green (−)/red (+) axis, b^* is the blue (−)/yellow (+) axis.

2.3. Coloration of plastics

In order to test the capacity of pigment samples to produce red hue, two pigment compositions: Mn 2 and Si 2 were chosen for the studies. Poly(methyl methacrylate) (PMMA) was used as the polymer matrix for fabricating the pigmented compact. PMMA is a known water soluble polymeric material extensively used for cold extrusion of many inorganic oxides such as alumina and zirconia. The pigment (10 wt.%) was ultrasonicated (Vibronics, 250 W, India) in an alcohol/water (1:4) mixture for 10 min. to ensure complete dispersion of the pigment particles. A viscous solution of PMMA (90 wt.%) was made using a conventional electrical coil heater. The pigment dispersion was slowly added with stirring and converted to a thick paste. The paste after 2 h curing was compressed uniaxially into a form of cylindrical discs using a hydraulic press (Lawrence & Maya, India) at a pressure of 25 MPa. Both sides of the pigmented polymer were lapped using a fine grade emery sheet for obtaining a polished surface. The intensity of the color of plastics will depend on the concentration of the pigment.

3. Results and discussion

3.1. Structural studies

The powder XRD patterns of the $Ce_{0.95}M_xPr_{0.05-x}O_2$ (M = Mn and Si, x ranges from 0 to 0.05) pigments are shown in Fig. 1. The intense and sharp peaks found in the diffraction patterns reveal the crystalline nature of the powders. All compounds crystallize with the cubic fluorite structure of CeO_2 (space group – $Fm3m$, No. 225) and all the peaks are in good agreement with the JCPDS card no. 34-394. Doping of small amounts of praseodymium and Mn/Si in cerium oxide retains the fluorite structure except minor variations in the d-spacings as expected.

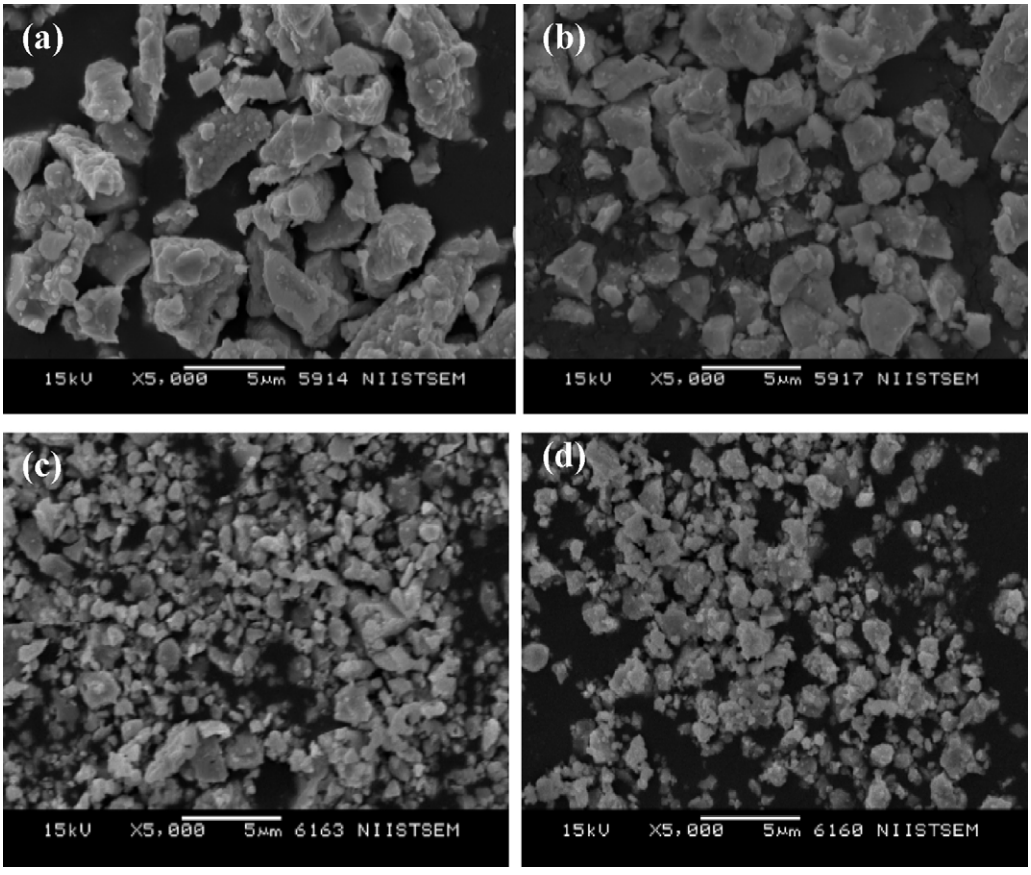

Fig. 2. SEM micrographs of (a) Mn 2, (b) Mn 3, (c) Si 2, and (d) Si 3 pigments. Si^{4+} co-doped Pr^{4+}–CeO_2 exhibits smaller particles compared to the Mn^{4+} co-doped ceria pigments.

Table 1
Color coordinates, chroma, hue angle and band gap of $Ce_{0.95}M_xPr_{0.05-x}O_2$ (M = Mn and Si, x ranges from 0 to 0.05). The band gap decreases with the incorporation of Mn^{4+}/Si^{4+} into the Pr–CeO_2 matrix.

Sample	L^*	a^*	b^*	C*	h°	E_g (eV)	ΔE^*
CP	44.25	18.35	15.49	24.01	40.16	1.88	–
Mn 1	37.64	20.75	15.11	25.67	36.06	1.86	7.0
Mn 2	38.33	21.96	16.19	27.29	36.39	1.88	6.9
Mn 3	41.89	21.41	17.17	27.44	38.72	1.87	4.2
Mn 4	47.88	17.61	16.11	23.86	42.45	1.90	3.7
Mn 5	56.85	2.61	2.60	3.69	44.81	2.78	23.9
Si 1	51.55	22.07	22.23	31.32	45.20	1.89	10.6
Si 2	50.70	25.85	24.73	35.78	43.72	1.87	13.5
Si 3	57.07	20.34	20.14	28.62	44.70	1.86	13.7
Si 4	55.88	20.03	18.32	27.14	42.44	1.84	12.0
Si 5	84.31	4.25	12.83	13.51	71.66	2.90	42.5

$C_{ab} = (a^{*2} + b^{*2})^{1/2}$, purity of hue (0–100) and $h_{ab} = \arctan(b^*/a^*)$, hue angle (red = 35°), $\Delta E^* = \sqrt{(\Delta a^{*2}) + (\Delta b^{*2}) + (\Delta L^{*2})}$.

3.2. Morphological and particle size analysis

The uniform particle size of the samples can be noticed from the SEM photographs (Fig. 2) of $Ce_{0.95}M_xPr_{0.05-x}O_2$ (M = Mn and Si, x ranges from 0 to 0.05) pigments. The particle size of Mn substituted pigments is found to be in the range 2–5 μm and that of Si substituted pigments in the range of 0.5–1 μm. Si^{4+} co-doped Pr^{4+}–CeO_2 exhibits smaller particles compared to the Mn^{4+} co-doped ceria pigments and this is clear from the increased lightness of the $Ce_{0.95}Si_xPr_{0.05-x}O_2$ (Table 1). The effective solid solution formation was checked by energy dispersive spectrophotometer (EDS) analysis attached with TEM. Fig. 3(a) and (b) shows the micrographs and EDS analysis of selected samples (Mn 2 and Si 2) and identifies the presence of all the expected elements. This also further confirms the homogeneity of the phase formed. The compositions derived from the micro-chemical analysis of the pigments are in close agreement with the stoichiometry of the formulae.

The particle size distribution and histogram of the Mn 2 and Si 2 pigments calcined at 1300 °C are illustrated in Fig. 4. Particle size analysis of the typical pigments Mn 2 and Si 2 reveals a mean diameter of 5.86 μm (size of 90% particles < 12.62 μm, 50% particles < 4.66 μm and 10% particles < 1.16 μm) and 5.57 μm (size of 90% particles < 10.08 μm, 50% particles < 5.08 μm and 10% particles < 1.44 μm), respectively. The histograms show that

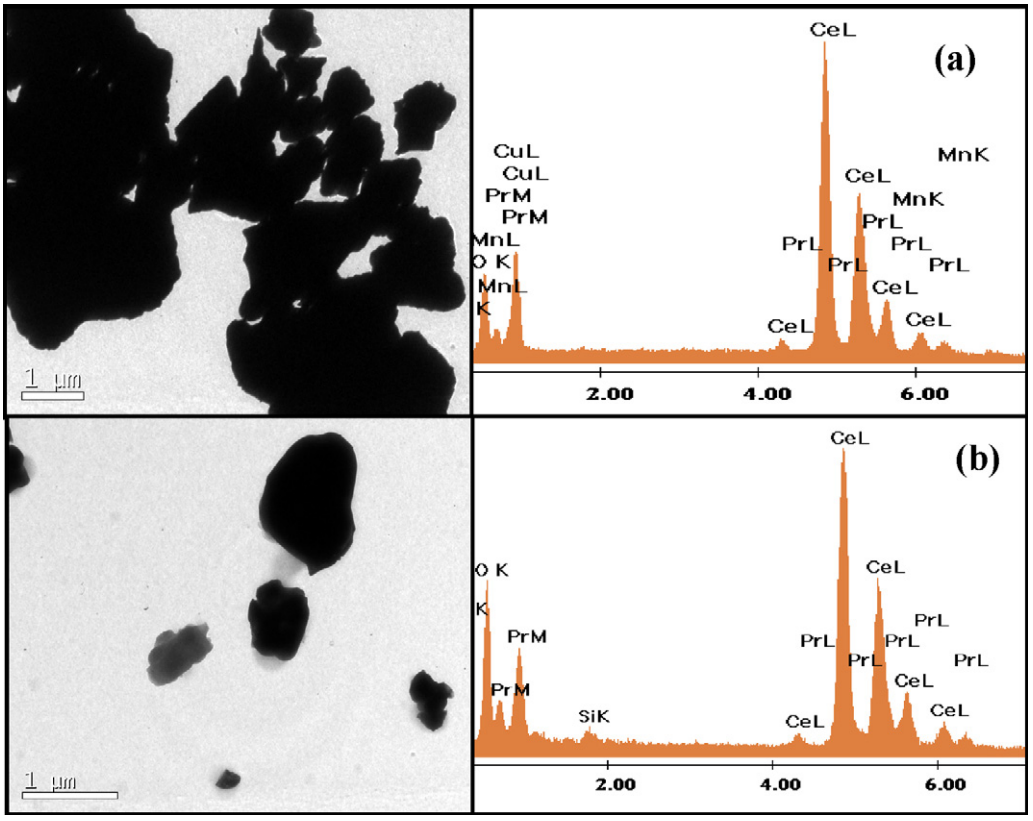

Fig. 3. Micrograph and EDS analysis of (a) Mn 2 and (b) Si 2 pigments and identifies the presence of all the expected elements.

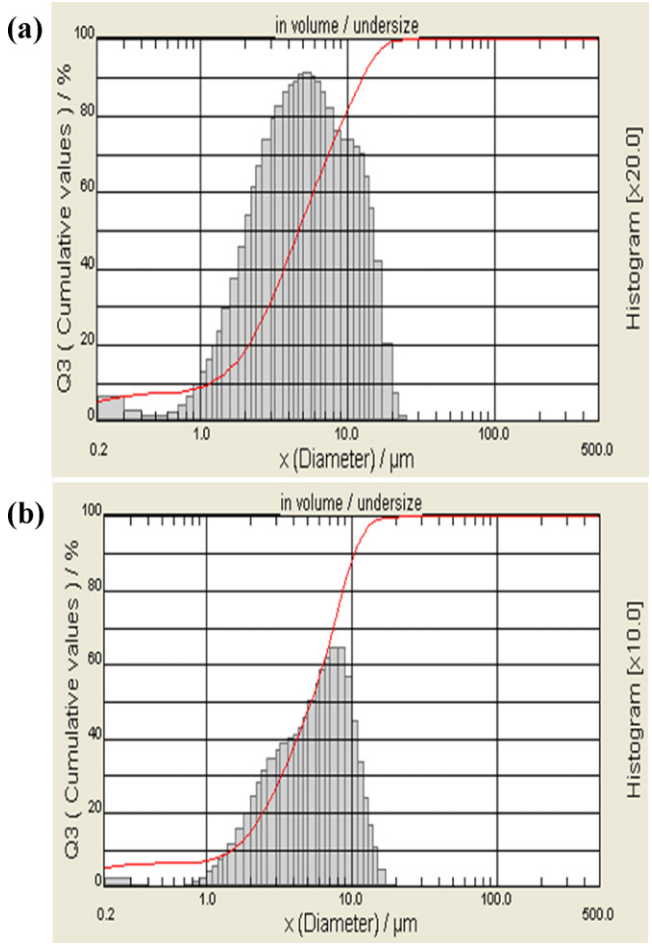

Fig. 4. Particle size distribution of (a) Mn 2 and (b) Si 2 pigments calcined at 1300 °C. Mn 2 and Si 2 reveals mean diameter of 5.86 μm and 5.57 μm, respectively.

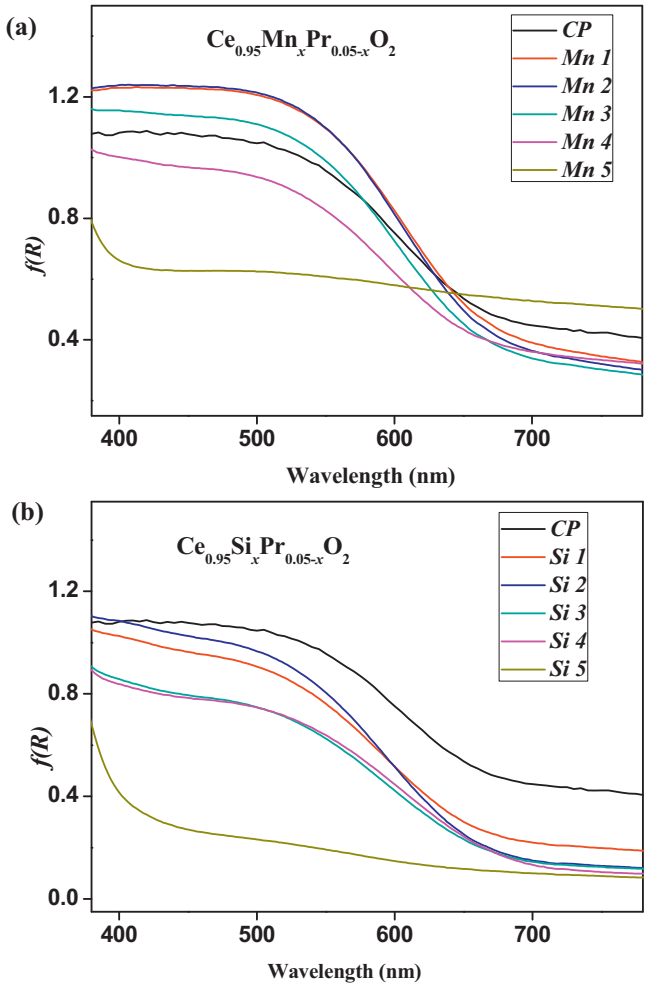

Fig. 5. Absorbance spectra of (a) $Ce_{0.95}Mn_xPr_{0.05-x}O_2$ and (b) $Ce_{0.95}Si_xPr_{0.05-x}O_2$ pigments. Si^{4+}substitution blue shifts the absorption edge of Pr-doped ceria and Mn^{4+} substitution stabilizes the absorption edge.

the greater particle size concentration (peak of highest intensity) for Mn 2 is in the fine particle region between 5 μm and 6 μm, whereas for Si 2 more particles are distributed in the region < 6 μm.

3.3. UV–vis spectroscopy

Absorbance spectra of CeO_2–PrO_2 system co-substituted with Mn and Si are shown in Fig. 5. In cerianite doped red pigments, the coloring mechanism is based on the shift of the charge transfer band of the semiconductor CeO_2 to higher wavelengths, introducing an additional electronic level by doping praseodymium. The 4f valence shell of Ce^{4+}([Xe]) in cerianite is empty, and that of O^{2-} ([Ne]$2s^2 2p^6$) is full: adjacent Ce^{4+} ions are virtually in contact in the fluorite lattice and, as a result, 4f orbitals overlap in a cationic conduction band; similarly, overlap of 2p orbitals of oxygen ions gives to an anionic valence band. The Ce–O bonds have a stronger ionic character, and hence a smaller contribution of the Ce 5d and 4f orbitals in the VB, in CeO_2 [25]. The band gap between the anionic band and the cationic band is 3.01 eV. By doping CeO_2 with Pr^{4+} ions, the $4f^1$ electron of the praseodymium valence shell introduces an additional electronic level of energy between the O^{2-} valence band and Ce^{4+} conduction band, and a reduced band gap of 1.88 eV is observed. The CeO_2 band gap falls in indigo region of visible wavelengths, and a complementary light yellow color is observed. By contrast, Pr^{4+}–CeO_2 absorbs in the wavelength region below 600 nm producing a red color [26].

The band gap energy (E_g) (Table 1) calculations reveal a substantial reduction in the band gap of $Ce_{0.95}M_xPr_{0.05-x}O_2$ when compared to CeO_2. Substitution of Mn^{4+}/Si^{4+} into CeO_2 lattice induces formation of intermediate energy levels in the CeO_2 semiconductor on either side of fermi level that cause a change in the band gap. The formation of mixed oxide alters the optical characteristics of the resultant material due to the contribution of Mn_{3d} and Si_{3p} to the conduction band. In the case of solid solution containing Mn^{4+}/Si^{4+} and Ce^{4+} the conduction band is formed by Ce_{4f} and Mn_{3d}/Si_{3p} resulting in the band gap widening (2.78/2.90 eV). As far as the effect of counter ions is concerned, Si co-doped pigments give practically the same spectra, with a blue shift in the absorption edge resulting in bright reddish brown hue. A gradual shift of CT band can be actually appreciated along with the increase in

concentration of Si in praseodymium doped ceria. Mn co-doped pigments show increased absorbance and results in dark brown hue. The width of the band gap is determined by the extent of overlap of the valence orbitals and by the difference between the electronegativities of the cations and anions involved [27–29]. The electronegativities of the metals only vary in small steps and the substitution of one metal by the other usually produces small shifts in elctronegativity difference and hence small change in bandgap is expected on co-substitution of Mn or Si with Pr in the cerianite lattice. As Si has higher electronegativity than Mn and Ce, the difference in electronegativity between the cations and oxygen decreases and more shift in absorption edge is expected for silicon co-doped samples than that of manganese containing compounds. The change in color of CP with increasing content of doped element accounts for the shift in absorption edge, which is caused by the change in chemical bonding nature by incorporating higher electronegative metal ion into the praseodymium–cerium matrix.

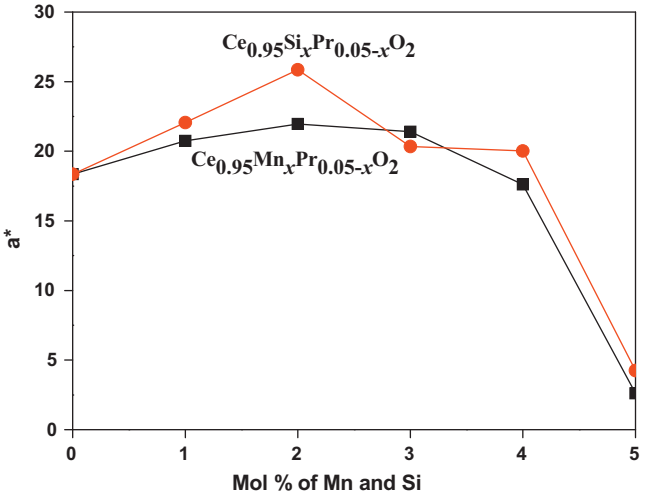

Fig. 6. Variation of a^* (redness) with manganese and silicon concentration. Si substitution enhances the redness of cerianite pigment whereas Mn substitution produces different shades of red.

3.4. Color characterization

The color of the synthesized pigments is numerically expressed in terms of the color co-ordinates (Table 1). The lightness (L^*) increases as the praseodymium content decreases and Mn and Si content increases in both the set of compositions. The redness (a^*) of Mn co-substituted $Ce_{1-x}Pr_xO_2$ compounds increases with increase in concentration of Mn, with low b^* values and hence the samples exhibit more dark brown color. For Si co-substituted $Ce_{0.95}Pr_{0.05}O_2$ compounds both a^* and b^* are almost same and exhibit bright reddish brown hue. The variation of redness (a^*) with manganese and silicon content is shown in Fig. 6. Increase in redness is obvious from the shift in the absorption edge of the Si^{4+} substituted samples (Fig. 5). In Mn^{4+} substituted Pr–CeO_2 the redness is stabilized with increase in concentration of manganese. These can account for the high value of total color difference (ΔE^*) in the case of silicon co-doped samples (Table 1). The parameters, a^* and b^* values decrease considerably for samples without praseodymium, which is responsible for the change of the color of the

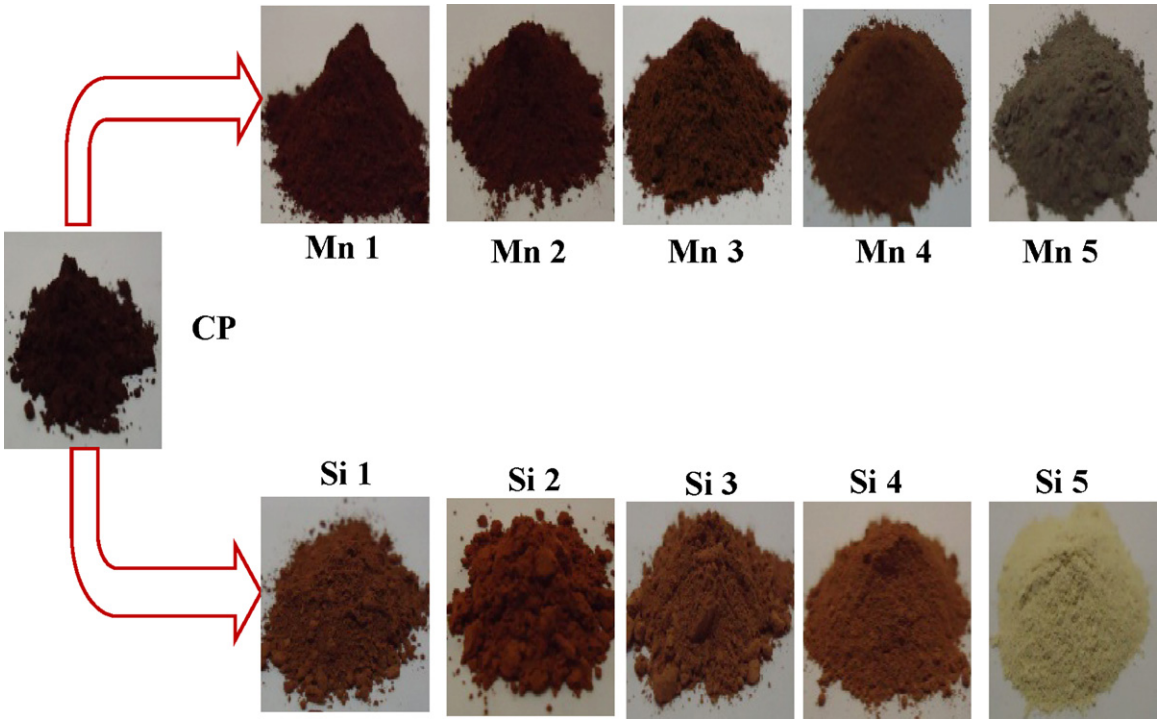

Fig. 7. Photographs of $Ce_{0.95}M_xPr_{0.05-x}O_2$ Mn^{4+}/Si^{4+} pigments. Color of the pigment change from bright reddish brown to bright cream for Si substituted ceria and dark brown to ash color for Mn substituted ceria. (For interpretation of the references to color in this figure legend, the reader is referred to the web version of the article.)

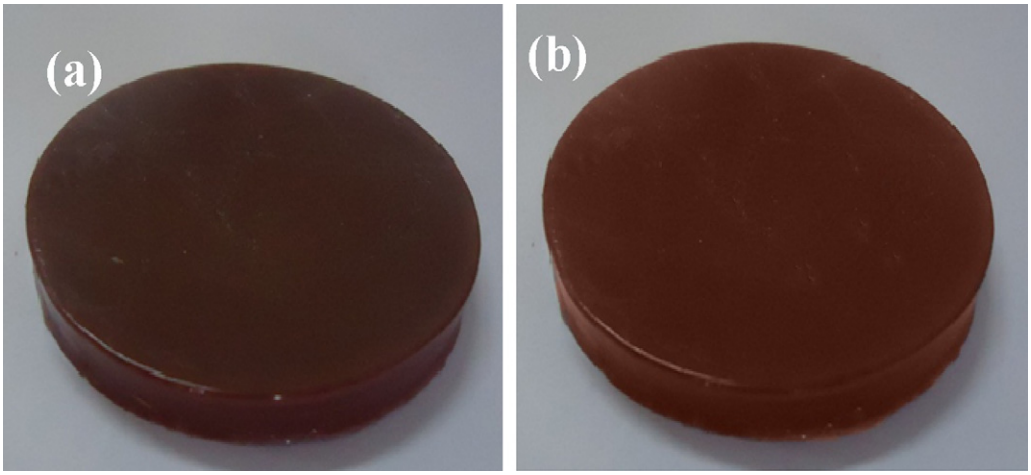

Fig. 8. Photographs of (a) Mn 2 (10%) + PMMA, and (b) Si 2 (10%) + PMMA. The test pieces exhibit uniform distribution of pigment particles in the polymer matrix.

pigment from dark brown via bright reddish brown to bright cream for Si substituted ceria and ash color for Mn substituted ceria (Fig. 7). The hue angle values reveal that the $Mn^{4+}$and Si^{4+} co-doped $Ce_{0.95}Pr_{0.05}O_2$ pigments lie in the brick red to dark-brown region of the cylindrical color space (h° = 0–35 for red and 35–70 for orange). It is clear from the $L^*a^*b^*$ values of the $Ce_{0.95}M_xPr_{0.05-x}O_2$ (M = Mn, Si) pigments summarized in Table 1 that the present values are significantly higher than recently reported praseodymium doped ceria powders (5% praseodymium doped CeO_2: $L^* = 66$; $a^* = 12$; $b^* = 9.5$), synthesized by microwave-assisted hydrothermal route [6].

3.5. Coloration of plastics

The coloring performance of the typically synthesized pigments (Mn 2 and Si 2) was tested for its coloring application in a substrate material like PMMA. Typically, 10 wt.% pigment sample was dispersed in PMMA and compressed to a cylindrical disc (Fig. 8). The color co-ordinates of the test pieces were measured at different locations. The $L^*a^*b^*$ values obtained were more or less the same indicating the uniform distribution of pigment particles in the polymer matrix.

4. Conclusions

The paper presents the preparation and optical properties of environmentally friendly pigments of reddish-brown hue based on $Ce_{0.95}M_xPr_{0.05-x}O_2$, (M = Mn and Si, x ranges from 0 to 0.05) solid solutions. The incorporation of Mn^{4+}/Si^{4+} into the CeO_2–PrO_2 system slightly shifted the color to dark brown and bright reddish brown by decreasing the band gap energies. Mn^{4+}/Si^{4+} incorporation in CeO_2–PrO_2 system offers to reduce the cost of the raw materials displaying different shades of dark brown and bright reddish brown hue. The above investigations suggest that these products have potential to be used as environmentally secure pigments for surface coating applications.

Acknowledgment

One of the authors, L.S. Kumari would like to acknowledge the Council of Scientific and Industrial Research for the financial support toward the Senior Research Fellowship.

References

[1] H.M. Smith, High Performance Pigments, Wiley-VCH, 2002.
[2] R.S. Pavlov, J.B.C. Castello, V.B. Marza, J.M. Hohembergerger, New red-shade ceramic pigments based on $Y_2Sn_{2-x}Cr_xO_{7-\delta}$ pyrochlore solid solutions, J. Am. Ceram. Soc. 85 (5) (2002) 1197–1202.
[3] I.G. Vasilyeva, B.M. Ayupov, A.A. Vlasov, V.V. Malakhov, P. Macaudiare, P. Maestro, Color and chemical heterogeneities of $\hat{I}^3$–[Na]–Ce_2S_3 solid solutions, J. Alloys Compd. 268 (1-2) (1998) 72–77.
[4] P. Rhone, 1.257.078 (1960).
[5] J.P. Chaminade, R. Olazcuaga, G. Le Polles, G. Le Flem, P. Hagenmuller, Crystal growth and characterization of $Ce_{1-x}Pr_xO_2$ ($x = 0.05$) single crystals, J. Cryst. Growth 87 (4) (1988) 463–465.
[6] F. Bondioli, A.M. Ferrari, L. Lusvarghi, T. Manfredini, S. Nannerone, L. Pasquali, G. Selvaggi, Synthesis and characterization of praseodymium-doped ceria powders by a microwave-assisted hydrothermal route, J. Mater. Chem. 15 (2005) 1061–1066.
[7] P. Sulcova, M. Trojan, Study of $Ce_{1-x}Pr_xO_2$ pigments, Thermochim. Acta 395 (2003) 251–255.
[8] M. Nahum, B. Hector, M. Raquel, J. Beatriz, B.C. Juan, E. Purificacion, Optimization of praseodymium-doped cerium pigment synthesis temperature, J. Am. Chem. Soc. 86 (2003) 425–430.
[9] S.T. Aruna, S. Ghosh, K.C. Patil, Combustion synthesis and properties of $Ce_{1-x}Pr_xO_{2-\delta}$ red ceramic pigments, Int. J. Inorg. Mater. 3 (2001) 387–392.
[10] P. Sulcova, M. Trojan, The synthesis of the $Ce_{0.95-y}Pr_{0.05}La_yO_{2-y/2}$ pigments, Dyes Pigments 44 (3) (2000) 165–168.
[11] P. Sulcova, The synthesis of $Ce_{0.95-y}Pr_{0.05}Nd_yO_{2-y/2}$ pigments, Dyes Pigments 47 (3) (2000) 285–289.
[12] P. Sulcova, M. Trojan, The synthesis and analysis of $Ce_{0.95-y}Pr_{0.05}Sm_yO_{2-y/2}$ pigments, Dyes Pigments 58 (1) (2003) 59–63.
[13] P. Sulcova, M. Trojan, Synthesis of $Ce_{1-x}Pr_xO_2$ pigments with other lanthanides, Dyes Pigments 40 (1) (1999) 87–91.
[14] R. Poulenc, 85.08611 (1960).
[15] M. Llusar, L. Vitaskova, P. Sulcova, M.A. Tena, J.A. Badenes, G. Monros, Red ceramic pigments of terbium-doped ceria prepared through classical and non-conventional coprecipitation routes, J. Eur. Ceram. Soc. 30 (1) (2010) 37–52.

[16] A. García, M. Llusar, J. Calbo, M.A. Tena, G. Monrós, Low-toxicity red ceramic pigments for porcelainised stoneware from lanthanide–cerianite solid solutions, Green Chem. 3 (2001) 238–242.
[17] C.K. Jørgensen, E. Rittershaus, Powder-diagram spectroscopic studies of mixed oxides of lanthanides and quadrivalents metals, Mat. Fys. Medd. K. Dan. Vidensk. Selsk. 35 (15) (1967) 1–37.
[18] L.S. Kumari, P.P. Rao, P. Koshy, Red pigments based on CeO_2–MO_2–Pr_6O_{11} (M = Zr and Sn): solid solutions for the coloration of plastics, J. Am. Ceram. Soc. 93 (5) (2010) 1402–1408.
[19] B.M. Reddy, A. Khan, P. Lakshmanan, M. Aouine, S. Loridant, J.-C. Volta, Structural characterization of nanosized CeO_2–SiO_2, CeO_2–TiO_2, and CeO_2–ZrO_2 catalysts by XRD, Raman, and HREM techniques, J. Phys. Chem. B 109 (8) (2005) 3355–3363.
[20] B.M. Reddy, A. Khan, Nanosized CeO_2–SiO_2, CeO_2–TiO_2, and CeO_2–ZrO_2 mixed oxides: influence of supporting oxide on thermal stability and oxygen storage properties of ceria, Catal. Surv. Asia 9 (2005) 155–171.
[21] A. Gupta, A. Kumar, Waghmare, V. Umesh, M.S. Hegde, Origin of activation of lattice oxygen and synergistic interaction in bimetal-ionic $Ce_{0.89}Fe_{0.1}Pd_{0.01}O_2$ catalyst, Chem. Mater. 21 (20) (2009) 4880–4891.
[22] L. Kepinski, D. Hreniak, W. Strek, Microstructure and luminescence properties of nanocrystalline cerium silicates, J. Alloys Compd. 341 (1-2) (2002) 203–207.
[23] T. Tago, S. Tashiro, Y. Hashimoto, K. Wakabayashi, M. Kishida, Synthesis and optical properties of SiO_2-coated CeO_2 nanoparticles, J. Nanopart. Res. 5 (1) (2003) 55–60.
[24] T. Masui, H. Tategaki, N. Imanaka, Preparation and characterization of SiO_2–CeO_2 particles applicable for environment-friendly yellow pigments, J. Mater. Sci. 39 (15) (2004) 4909–4911.
[25] F. Goubin, X. Rocquefelte, M.-H. Whangbo, Y. Montardi, R. Brec, S. Jobic, Experimental and theoretical characterization of the optical properties of CeO_2, $SrCeO_3$, and Sr_2CeO_4 containing $Ce^{4+}(f^0)$ ions, Chem. Mater. 16 (4) (2004) 662–669.
[26] R. Olazcuaga, G. Le Polles, A. El Kira, G. Le Flem, P. Maestro, Optical properties of $Ce_{1-x}Pr_xO_2$ powders and their applications to the coloring of ceramics, J. Solid State Chem. 71 (2) (1987) 570–573.
[27] M. Jansen, H.P. Letschert, Inorganic yellow-red pigments without toxic metals, Nature 404 (6781) (2000) 980.
[28] J.C. Philips, Bonds and bands in semiconductors, New York Academy Press, New York, 1973.
[29] C.K. Jorgensen, Oxidation Numbers and Oxidation States, Springer, Berlin, 1969.